

Multi-surface strength model for concrete beam-column joints subjected to cyclic loading

S.C. Fan & Z.N. Yin

School of Civil and Environmental Engineering, Nanyang Technological University, Singapore.

ABSTRACT: Laboratory tests of structural elements, in particular the reinforced concrete beam-column joints, subjected to cyclic loading provide useful information of the structural damage and post-damage ductile behaviour during an earthquake. With the advent of computer technology, it is possible to study the complicated phenomena through numerical simulations. However, the major hindrance lies in the establishment of a sound constitutive model for concrete. This paper puts in place a multi-surface strength model for concrete, which accounts for the elastic, plastic, damage and post-damage behaviour. It is a semi-theoretical model, in which the strength envelope is derived from experimental meridians and completed through strength theory. Different from those popular but over-simplistic strength criteria, such as Tresca and Mises, the present strength model takes into account all stresses. Eventually, the strength model is presented in multi-surface form in the 3-dimensional stress space (p -space) for different phases. The key one is the maximum strength surface, which is subsequently used to derive the elastic-limit surface and series of plastic loading surfaces. In addition, evolution of stress states is governed by known rules for the loading-unloading-reloading processes. In the pre-damage phase, non-associate plasticity and hardening rule are employed to govern the behaviour of concrete. In the post-damage phase, anisotropic damage theory is used to describe the stiffness degradation. The numerical simulation of a beam-column joint is presented and compared with experimental results.

Key word: Strength theory, Concrete, Constitutive law, Cyclic loading

1 INTRODUCTION

Beam-column joints are critical to the integrity of a structure because they ensure continuity of a structure and transfer forces from one element to another. During a moderate to strong seismic excitation, the strength of a beam-column joint is expectedly stretched towards or even beyond its ultimate limit. Very often, a single occurrence of such beyond-the-limit event does not bring down the whole structure. The joints or other members may be partially damaged, and their strengths are weakened. Upon subsequent unloading and re-loading, the residual strength is further weakened till failure. For a reinforced concrete (RC) beam-column joint, such degradation phenomenon of residual strength has long been recognized but it has not been understood precisely. In an RC joint, the concrete material is in various three-dimensional stress states, which are very complicated. Post-mortem of disastrous collapse of a building structure often points finger to the weakness of the joints. It can be traced to the poor understanding of the characteristic that reinforced concrete exhibits under reversed cyclic loading. Even with the advent of computer technology and the maturity of numerical techniques, precise simulation of response of RC joint to cyclic loading remains a challenge to the engineering community. The success now hinges on the thorough understanding and proper modelling of the concrete material behaviour. Apart from the need for intricate numerical procedures, it demands a constitutive model capable to reflect various phenomena ranging from linear elastic recovery to non-linear plastic flow and series of damage states. The task includes the establishment of demarcation limits, which mark the transition between distinct behaviours such as elastic to plastic, or plastic to

partial damage, etc. A wealth of constitutive models can be found in the literature. Amongst them, non-linear elasticity models have a long history (Evans and Pister 1966; Kupfer and Gerstle 1973; Elwi and Murray 1979); plasticity models enjoys continuous development (Chen and Chen 1975; Murry et al 1979; Hsieh-Ting-Chen 1982; Vermeer and de Borst 1984; Han and Chen 1985; Simo et al 1988); more recently came various damage models (Frantziskonis and Desai 1987; Simo-Ju 1987; Mazars 1989; Yamaguchi and Chen 1990); and fracture models are also well received (Dougill 1976; Bazant and Kim 1979).

Each of the above-mentioned models explored to a great extent in certain aspects. Applications to some specific scenarios show great success. For example, the early biaxial plasticity models by Kupfer and Gerstle (1973) reflect only the 2D characteristics, while the triaxial models (Kotsovos and Newman 1979, Ottosen 1979, Willam and Warnker 1975, etc) yields good predictions of 3D behaviour at low hydrostatic (mean) pressures. Other developments include coupling models such as the elastic-plastic models (Chen-Chen, 1975; Murry, 1979; Hsieh-Ting-Chen, 1982; Pietruszczak-Jiang-Mirza, 1988; Han-Chen, 1985), which have emphasis on the hardening response of plain concrete. Successful plastic-damage or plastic-fracture coupling models were also reported.

This paper presents an elastic-plastic-damage model with emphasis on the demarcation surfaces defined in the 3D stress space (π -space), and its applications for cyclic loading. The key surface is the maximum strength surface, which demarcates the pre- and post damage phases. It is subsequently used to derive the elastic-limit surface and series of plastic loading surfaces. In addition, evolution of stress states is governed by known rules for the loading-unloading-reloading processes. In the pre-damage phase, non-associate plasticity and hardening rule are employed to govern the behaviour of concrete. In the post-damage phase, anisotropic damage theory is used to describe the stiffness degradation (or softening). Numerical simulation is included, and its validity is demonstrated through comparisons with available experimental results.

2 MULTI-SURFACE STRENGTH MODEL

In the present model, demarcation surfaces are defined in the 3D stress space. The first is the elastic limit surface that is the envelope to all admissible elastic stress states. Beyond that, the stress state becomes plastic. The second is the maximum strength surface that is the boundary limit to all admissible plastic stress states. Upon reaching the maximum stress state, damage begins to creep in and the strength starts weakening. Though it may survive on further damages, it suffers more degradation of strength (or stiffness). Ultimate failure occurs when the ultimate residual strength is exceeded. What follows will describe the construction of the surfaces and the governing rules in different demarcated zones.

2.1 Maximum strength surface

The maximum strength surface is defined first. For all conventional materials including concrete, the shape must be convex and smooth (e.g. paraboloidal). In general, available models can be classified under two categories: i) postulate surface based on simple theories that include Rankine (1867), Tresca (1864), Mises (1913), Mohr-Coulomb (1900), Drucker-Prager (1952); ii) regression surface of experimental data such as Kotosvos and Newman (1979), Ottosen (1979), Willam and Warnker (1979), Hsieh-Ting-Chen (1982) etc. Although models under the first category are derived from some basic physical parameters, very often they are found not applicable beyond a limited range of stress states. Against this background, we adopt a strategy of semi-empirical and semi-theoretical way to construct the surface. Skeleton curves are obtained empirically and put in place, and then the whole surface is completed via 3D strength theory. It was known and proved theoretically that the strength surface is 6-fold (6-sectorial) symmetric about the hydrostatic axis. In other words, the whole surface is a continuous repeated pattern of a typical 60° sectorial surface. Plenty of experimental data are available for the maximum stress states at 0° and 60° , which correspond to the stress states along the tensile and compressive meridians respectively. A pair of meridians is chosen (e.g. Kosotvos), and then the 60° -sectorial surface is completed via UTSS theory (Yu 1999). In the UTSS theory, a 3D strength criterion is established using two shear parameters and a unified weighted parameter 'b', thus

called Unified Twin Shear Strength theory. The construction details can be found in literature (Fan et al 2002). In brevity, the two-step formulae are shown below.

Step 1: Tensile and compressive meridian: r_t and r_c

$$r_t = 1.0964 \left(0.05 - \frac{1}{\sqrt{3}} \theta \right)^{0.857} \quad \theta = 0^\circ \quad (1a)$$

$$r_c = 1.635 \left(0.05 - \frac{1}{\sqrt{3}} \theta \right)^{0.724} \quad \theta = 60^\circ \quad (1b)$$

here the surface is expressed in Haigh-Westergaard coordinate $(\mathbf{x}, r, \mathbf{q})$ (Owen and Hinton, 1980), i.e.

$$\mathbf{x} = \frac{1}{\sqrt{3}f_c} (\mathbf{s}_1 + \mathbf{s}_2 + \mathbf{s}_3) \quad (1c)$$

$$r = \frac{1}{\sqrt{3}f_c} \sqrt{(\mathbf{s}_1 - \mathbf{s}_2)^2 + (\mathbf{s}_1 - \mathbf{s}_3)^2 + (\mathbf{s}_2 - \mathbf{s}_3)^2} \quad (1d)$$

where f_c is uni-axial compressive strength of concrete.

Step 2: 60°-sectorial surface between r_t and r_c in terms of the weighted twin-shear parameter 'b'

$$r_f = \frac{r_t r_c \sin 60^\circ}{r_t \sin \theta + r_c \sin(60^\circ - \theta)} (1-b) + b \frac{r_t}{\cos \theta}, \quad \text{when } 0^\circ \leq \theta \leq \theta_b \quad (2a, 2b)$$

$$r_f = \frac{r_t r_c \sin 60^\circ}{r_t \sin \theta + r_c \sin(60^\circ - \theta)} (1-b) + b \frac{r_c}{\cos(60^\circ - \theta)}, \quad \text{when } \theta_b \leq \theta \leq 60^\circ$$

2.2 Elastic limit surface

The elastic limit surface is defined as a diminished replica ($k_0=50\sim 60\%$) of the maximum strength surface.

2.3 Governing rules for loading path between the elastic limit and maximum surfaces

i) Hardening rule

Beyond the elastic states, the stress path is associated with the development of the effective plastic strain e_p . For each plastic strain value, the corresponding stress states form a surface called 'loading surface'. Its shape matches precisely the shape of the elastic limit surface when the plastic strain is zero, and expands non-uniformly with increasing strain till reaching the maximum strength surface. Hence, a loading surface can be written as follows (Chen, W. F., 1982).

$$f(\mathbf{s}) = r - k r_f = 0 \quad (3)$$

where k denotes the hardening parameter, which is a function of the effective plastic strain. The zero plastic strain corresponds to $k=k_0$ (on the elastic limit surface); and maximum plastic strain corresponds to $k=1$ (on the maximum strength surface).

ii) Non-associate flow rule for stress-strain relationship

It has been recognized that the associate flow rule often over-estimates the volumetric dilation of concrete. The non-associate flow rule is more appropriate. Derivation of the stiffness matrix \mathbf{D}_{ep} can be found in standard textbook. It can be written as follows.

$$\mathbf{D}_{ep} = \mathbf{D}_e - \frac{\mathbf{D}_e \frac{\partial f}{\partial \mathbf{s}} \frac{\partial \mathbf{g}}{\partial \mathbf{s}} \mathbf{D}_e}{\frac{\partial f}{\partial \mathbf{s}} \mathbf{D}_e \frac{\partial \mathbf{g}}{\partial \mathbf{s}} + Y \sqrt{\left(\frac{\partial \mathbf{g}}{\partial \mathbf{s}} \right)^T \frac{\partial \mathbf{g}}{\partial \mathbf{s}}}} \quad (4)$$

in which \mathbf{D}_e is the elastic stiffness matrix, γ is a strain-related coefficient ($=\gamma/\gamma_p$), f is the yielding function defined by Equation (3), and g is the plastic potential function defined as follows (Yu et al 1999).

$$\mathbf{g} = \mathbf{s}_1 - \frac{\mathbf{a}^*}{l+b} (b\mathbf{s}_2 + \mathbf{s}_3) = \mathbf{s}_1, \quad \text{when } \mathbf{s}_2 \leq \frac{\mathbf{s}_1 + \mathbf{a}^* \mathbf{s}_3}{l + \mathbf{a}^*} \quad (5a)$$

$$\mathbf{g} = \frac{l}{l+b} (\mathbf{s}_1 + b\mathbf{s}_2) - \mathbf{a}^* \mathbf{s}_3 = \mathbf{s}_1, \quad \text{when } \mathbf{s}_2 \geq \frac{\mathbf{s}_1 + \mathbf{a}^* \mathbf{s}_3}{l + \mathbf{a}^*} \quad (5b)$$

where $\mathbf{a}^* = (1 - \sin \gamma) / (1 + \sin \gamma)$ and γ denotes the frictional angle.

2.4 Residual strength in the post-damage phase

Upon reaching the maximum stress state, damage begins to creep in and the strength starts weakening. Though it may survive on further damages, it suffers more degradation of the strength. The damaged material is considered as a new material having a reduced maximum strength, namely ‘residual strength’. As damage continues, the progressive damage states can be represented by a series of reducing residual strengths, each of which associates with a set of damage scalars ($\gamma_1, \gamma_2, \gamma_3$). The scalar γ_i ($i=1,3$) measures the extent of damage in the i^{th} principal direction. It varies between 0 and 1. When all γ_i equals to 0, no damage occurs and the stress state corresponds to one on the maximum strength surface. On the other hand, as all γ_i equals to 1, the material is totally damaged with zero residual strength. In the current study, the damage scalar adopts Mazars’ (1989) two-parameter model, which governs the progressive damages. The damage scalar is determined by the strain ratio (e/e_D) and the excess of ($e - e_D$), in which e_D denotes the strain at maximum stress. Note that the damaged concrete material is no longer isotropic.

3 ALGORITHM FOR REVERSE LOADING AND RELOADING

In the case of cyclic loading, we have to consider not only the loading path but also the reverse loading and reloading paths. For each incremental change, it leads to a corresponding change in stress state. Each new state associates with a new point in the p -space either on an elastic surface ($\mathbf{k} < \mathbf{k}_0$) or a loading surface ($\mathbf{k}_0 < \mathbf{k} < 1$) or a new damage state (e/e_D). In the pre-damage phase, there are three possible scenarios, i.e. $\Delta \mathbf{k} < 0, \Delta \mathbf{k} = 0, \Delta \mathbf{k} > 0$. The governing rules remain the same as those for loading path except that the unloading/reloading path is ruled by the elastic stress-strain relation \mathbf{D}_e if the effective plastic strain is less than the maximum e_p (or the associated \mathbf{k}) reached in history. The procedures are described in the algorithm below. In the computer coding, the loading increment/decrement is implemented by displacement control, which associates with an incremental strain γe_n . The updated stress state can be obtained from the current stress state \mathbf{s}_n and strain e_n as follows.

Subroutine ($\mathbf{s}_n, e_n, \gamma e_n, \mathbf{D}_e, \kappa_n, \epsilon_p$)

Use Eq. (3), \mathbf{s}_n yields a corresponding hardening parameter \mathbf{k}_n , namely $(\kappa_n)_1$

Use Eq. (3), $(\mathbf{s}_n + \mathbf{D}_e \gamma e_n)$ yields another corresponding hardening parameter \mathbf{k}_n , namely $(\kappa_n)_2$

if $(\kappa_n)_1 < (\kappa_n)_2$ (i.e. reloading procedure) then

if $(\kappa_n)_1 < (\kappa_n)_2 < \max(\kappa)$ then

elastic reloading, $\mathbf{s}_{n+1} = \mathbf{s}_n + \mathbf{D}_e \gamma e_n$

else

if $\max(\kappa) < (\kappa_n)_1 < (\kappa_n)_2 < 1.0$ then

plastic reloading, $\mathbf{s}_{n+1} = \mathbf{s}_n + \mathbf{D}_{ep} \gamma e_n$

else ($\kappa_n > 1.0$)

anisotropic damage be considered

end

end

else (i.e. reverse loading procedure)

if $(e_p < \max(e_p))$ then

elastic unloading $\mathbf{s}_{n+1} = \mathbf{s}_n + \mathbf{D}_e \gamma e_n$

```

else
  if(not yet reach the maximum strength surface) then
     $S_{n+1} = S_n + D_{ep} \cdot e_n$ 
  else
    anisotropic damage be considered
  end
end
end
end

```

In the post-damage phase, stiffness degradation occurs. The stiffness diminishes with increasing value of the damage scalars embedded in the stiffness matrix. In the process of reverse loading or reloading, the stress-strain relationship is ruled by the degraded stiffness.

4 NUMERICAL EXAMPLE

The present model is employed to simulate a reinforced concrete beam-column joint subjected to cyclic loading. We adopt the same geometrical and material parameters as those in the experiment done by Tsonos et al (1992). The configuration is shown in Figure 1. In the numerical model, truss-type and eight-node brick-type elements are used to model the steel reinforcement bars and concrete material respectively. Interface elements are put in place to account for the bond-slip effect between steel bar and concrete. Relationship between shear stress and bond-slip is approximated in according with the CEP-FIP model code (CEB-FIP 1993). Figure 2 shows the finite-element meshes for concrete and steel respectively.

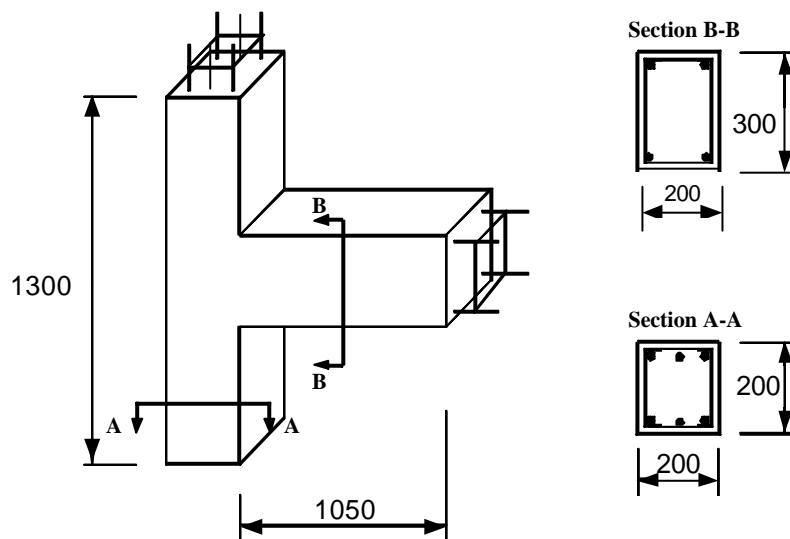
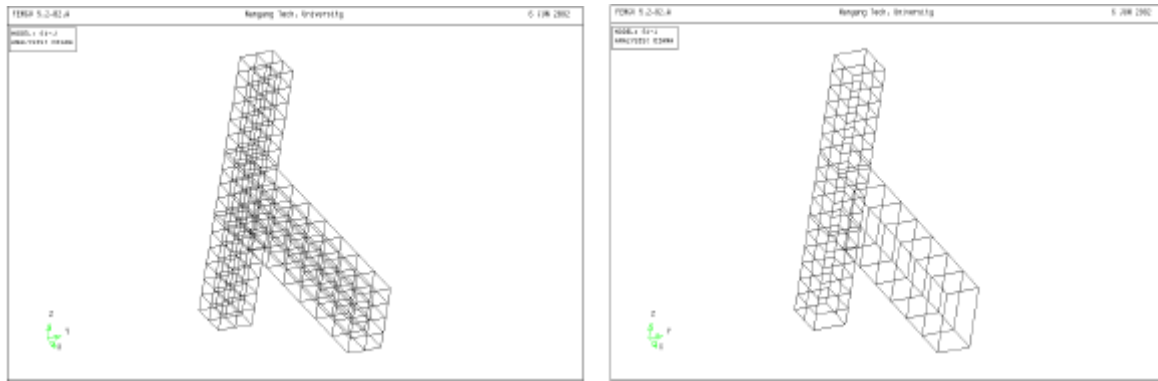


Figure 1 Configuration of the reinforced concrete beam-column joint

The material parameters are as follows. For concrete: Young's modulus $E_{con} = 21.0 \text{ GPa}$, uni-axial compressive strength $f_c = 36.98 \text{ MPa}$, uni-axial tensile strength $f_t = 3.4 \text{ MPa}$, Poisson's ration $\nu = 0.2$; for steel bars: Young's modulus $E_{steel} = 180.5 \text{ GPa}$.

The numerical results are plotted in Figure 3 and compared with the experimental results. They agree fairly well.



(a) Concrete model

(b) Reinforcement model

Figure 2 Finite element meshes

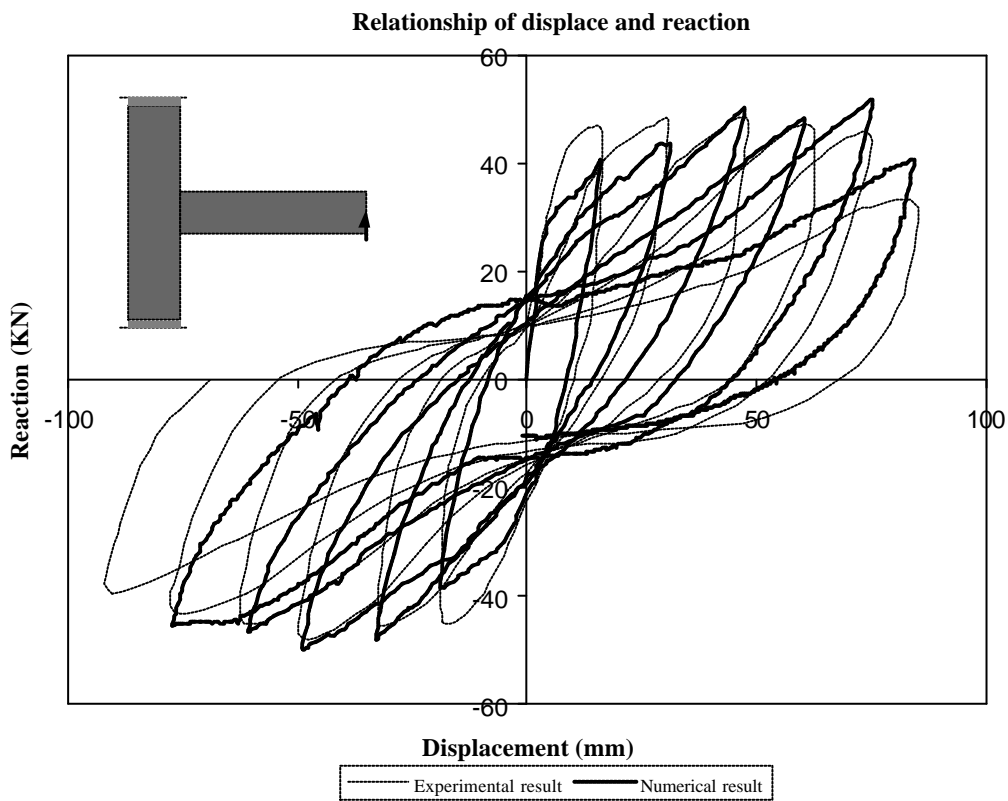


Figure 3 Comparison of experimental and numerical results

5 CONCLUSIONS

In this paper, a multi-surface strength model is presented, particularly for concrete material. It accounts for the elastic, plastic, damage and post-damage behaviour. The distinct feature is its semi-theoretical derivation, in which the strength envelope is derived from experimental meridians and completed through strength theory. Evolution of stress states is governed by known rules for the loading-unloading-reloading processes. In the pre-damage phase, non-associate plasticity and hardening rule are employed to govern the behaviour of concrete. In the post-damage phase, anisotropic damage theory is used to describe the stiffness degradation. Its capacity is demonstrated in the numerical simulation of a reinforced concrete beam-column joint subjected to cyclic loading.

6 REFERENCE

- Bazant, Z.P. & Kim, Sang-Sik. 1979. Plastic-fracturing theory for concrete, *J. Engrg. Mech. Div., ASCE*, Vol 105(3) 151-163
- CEB-FIP model code 1990, design code (1993)*, Thomas Telford, Lausanne, Switzerland.
- Chen, A.C.T & Chen, W.F. 1975. Constitutive relations for concrete, *J. Engrg. Mech. Div., ASCE*, Vol 101(2) 265-481
- Chen, W.F. 1982. Plasticity on reinforced concrete. *McGraw-Hill Book Co.*, New York, N. Y. 379-380
- Dougill, J.W. 1976. On stable progressive fracturing solids, *J. of Applied Mathematics and Physics*, Vol 27 31-52
- Elwi, A.A. & Murry, D.W. 1979. A 3D hypoelastic concrete constitutive relationship, *J. Engrg. Mech. Div., ASCE*, Vol 105(4) 623-641
- Evans, R.J. & Pister, K.S. 1966. Constitutive equations for a class of nonlinear elastic solids, *Int. J. Solids Struct.*, Vol 2 427-455
- Fan, S.C. & Wang, F. 2002. A new strength criterion for concrete, *ACI Structural Journal*, Vol 99(3) 317-326
- Frantziskonis, G. & Desai, C.S. 1987. Constitutive model with strain softening, *Int. J. Solids Struct.*, Vol 23(6) 733-750
- Han, D.J. & Chen, W.F. 1985. A nonuniform hardening plasticity model for concrete materials, *Mech. Mat.*, Vol 4 283-302
- Hsieh, S. S., Ting E. C. & Chen, W. F. 1982. A plasticity-fracture model for concrete, *Int. J. Solids Struct.*, Vol. 18(3) 181-197
- Kotsovos, M.D. 1979. Mathematical description of the strength properties of concrete under generalized stress, *Magazine of Concrete Research*, Vol 31(108) 151-158
- Kupfer, H.B. & Gerstle, K.H. 1973. Behaviour of concrete under biaxial stresses, *J. Engrg. Mech. Div., ASCE*, Vol 99(4) 852-866
- Mazars, J. & Pijaudier-Cabot. 1989. Continuum damage theory – application to concrete, *Journal of Engineering Mechanics*, Vol 115(2) 345-365
- Murry, D.W., et al. 1979. A concrete plasticity theory for biaxial stress analysis, *J. Engrg. Mech. Div., ASCE*, Vol 105(2) 265-481
- Ottosen, N.S. 1977. A failure criterion for concrete, *ASCE Journal of Engineering Mechanics*, Vol 103(EM4) 527-535
- Owen, D.R.J. & Hinton, E. 1980. Finite element in plasticity: theory and practice, 301-302 Swansea: Pineridge Press
- Pietruszczak, S., Jiang, J. & Mirza, F.A. 1988. An elasto-plastic constitutive model for concrete. *Int. J. Solids and Structures*, Vol 24 (7) 705-722
- Simo, J.C. & Ju, J.W. 1987. Strain- and stress-based continuum damage models-I. Formulation, *Int. J. Solids Struct.*, Vol 23(7) 495-521
- Simo, J.C., Ju, J.W., Pister, K.S. & Taylor, R.L. 1988. Assessment of cap model: consistent return algorithms and rate-dependent extension, *J. Engrg. Mech. Div., ASCE*, Vol 114(2) 191-128
- Tsonos, A.G., Tegos, I.A. & Penelis, G.Gr. 1992. Seismic resistance of type 2 exterior beam-column joints reinforced with inclined bars, *ACI Structural Journal*, Vol 89(1) 3-12
- Vermeer, P.A. & de Borst, R. 1984. Non-associate plasticity for soils, concrete and rock, *Heron*, Vol 29 102-114
- Willam, K. J. & Warnker, E. P. 1975. Constitutive models for the triaxial behaviour of concrete, *IABSE Proceeding*, Vol. 19 1-31
- Yamaguchi, E. & Chen, W.F. 1990. Cracking model for finite element analysis of concrete materials, *Int. J. Solids Struct.*, Vol 106(5) 1242-1260
- Yu, M.H., Yang, S.Y. & Fan, S.C. 1999. Unified elasto-plastic associated and non-associated constitutive model and its engineering applications, *Computers and Structures*, Vol 71 627-636